Surface ordering and finite-size effects in liquid-crystal films

Hao Li, Maya Paczuski, Mehran Kardar, and Kerson Huang

Department of Physics, Massachusetts Institute of Technology, Cambridge, Massachusetts 02139

(Received 25 April 1991)

Motivated by recent experiments on liquid-crystal films, we study the development of heat-capacity singularities with the number of layers, n. With enhanced surface couplings, there are distinct peaks due to *surface* ordering and *bulk* ordering, at temperatures $T_S(n)$ and $T_B(n)$, respectively. Comparing exact results from the two-dimensional Ising model with a mean-field theory, we find in both cases that the evolution of the peaks is controlled by a length scale ξ_S for decay of surface order into the bulk. The bulk transition temperature is governed by a scaling function $F_S(n/\xi_S)$, which decreases with n for $n < \xi_S$, but increases with n for $n > \xi_S$. Qualitative trends for thin films agree well with experimental observations.

I. INTRODUCTION

Layered materials of finite thicknesses are important to many physical applications; high T_C superconducting films, liquid-crystal films, and helium films provide a few examples. Apart from practical applications, these systems are important experimental testing grounds for theories of two-dimensional (2D) physics. For example, the universal jump of superfluid density[1] in helium films is a consequence of the Kosterlitz-Thouless theory of unbinding of vortices,[2,3] while diffraction patterns from liquid-crystal films[4] have supported the prediction of an intermediate hexatic phase.[5] Recently, improvements in experimental technique have made it possible to study free-standing liquid-crystal films with thicknesses varying from several to thousands of layers.[6-9] Such substrate-free films are ideal for studying both two-dimensional behavior and crossover effects to three dimensions. A number of experiments have been carried out, among them precise measurements of heat capacity[7-9] and diffraction patterns.[6] The diffraction experiments reveal suppressed fluctuations in the displacement of surface particles.[6] The observation of two peaks in heat-capacity measurements indicates that the surface of the film develops bond orientational order prior to the bulk.[7-9] Together, these experiments suggest that couplings on and near the surface are stronger than those in the interior. Such an effect is common in thin films due to the surface tension between boundary layers[6] and the surrounding gas.

There is considerable literature dealing with both finite-size effects in films[10] and surface phase transitions.[11,12] While these studies focus mainly on the general aspects of finite-size scaling and critical behavior at surfaces, a precise knowledge of how the stronger surface couplings alter the usual finite-size effect (e.g., the shifting of the pseudocritical temperature) is still lacking. The experimentally observed[7-9] appearance and systematic shifting of the two peaks in the heat capacity, as the system crosses over from 2D to 3D behavior, certainly needs better understanding. To gain some information, we examine the heat capacity of several layered anisotropic models in this paper. Consider the general Hamiltonian

$$\mathcal{H} = \sum_{\alpha=1}^{n} \sum_{\langle i,j \rangle} J_H^\alpha \mathbf{S}_i^\alpha \cdot \mathbf{S}_j^\alpha + \sum_{\alpha=1}^{n-1} \sum_{i} J_V^\alpha \mathbf{S}_i^\alpha \cdot \mathbf{S}_i^{\alpha+1} , \quad (1.1)$$

where $\mathbf{S}_i^\alpha$ is a spin representing an order parameter at site i in the αth layer. Since we are interested in the general trends for T_C and C_V, rather than the precise critical exponents, we shall examine different order parameters. For the hexatic transition of liquid-crystal films[4] a two-component XY spin is appropriate,[5] but in order to obtain exact results we shall consider an Ising model.

There are many coupling constants in the above Hamiltonian. For simplicity, we restrict ourselves to four different coupling constants: J_S, the in-layer coupling on the surface; J_{SV}, the interlayer coupling from a surface to its neighbor; and J_H and J_V, the in-layer and interlayer couplings in the bulk. A schematic diagram of such a layered system is shown in Fig. 1. (For a finite-size scaling study of thick films, we set $J_{SV} = J_V$, and restrict ourselves to three different couplings.) We find that due to stronger surface couplings, there is a length scale ξ_S for decay of the surface order into the bulk. The usual finite-size scaling behavior for large n is altered for $n \sim \xi_S$, and there is a new scaling function governing the pseudocritical temperature, with scaling variable $x = n/\xi_S$. In the limit $x \to \infty$, this surface length scale decouples from the bulk, and the usual finite-size scaling behavior is recovered. For films of only a few layers, we use the model with four couplings, to get qualitative agreement with experiments.

The paper is organized as follows. In Sec. II we briefly summarize recent heat-capacity measurements on liquid-crystal films, and discuss the behavior of observed peaks. In Sec. III we investigate the Ising model on a two-dimensional strip. Using an exact expression for the partition function, the heat capacity is evaluated numerically, and the surface length scale and associated scaling function is obtained. In Sec. IV we examine the mean-field equations for layered systems both analytically and numerically, and find results similar to the Ising case. From the similarity of the two extreme treatments (including or neglecting fluctuations), we speculate that the basic trends are common to all layered systems with

J_S

n

$\leftarrow J_{SV}$

n−1

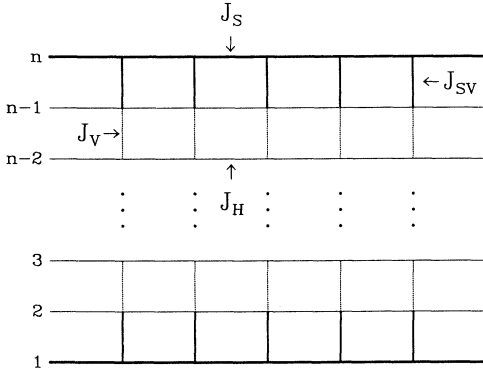$J_V \rightarrow$

n−2

$\uparrow$ J_H

3

2

1

FIG. 1. Schematic representation of the layered system with four couplings.

strong surface couplings. We conclude and suggest some possible directions for future work in Sec. V. The full expression for the partition function of the Ising model with four couplings on a strip, and a proof of a duality relation for the heat capacity, are presented in Appendixes A and B, respectively.

II. DISCUSSION OF EXPERIMENTS

Several recent experiments have yielded precise measurements of the heat capacity of liquid-crystal films, in the temperature range where the system undergoes a hexatic to liquid phase transition.[7-9] These experiments reveal two peaks in the heat capacity; the higher temperature peak is associated with surface ordering and the lower one with bulk ordering. Here we summarize the evolution of peak positions with film thickness in the two extreme limits.

A. Thin films (n ~ 3–10)

The two peaks approach each other as $n \rightarrow 4$, and change their relative weights, the surface peak getting more pronounced. The separation of their positions has been fitted to a simple formula $T_S(n) - T_B(n) \sim (n-4)^\Phi$, with $\Phi = 0.43$. The single peak for three layers shifts to significantly higher temperatures, and the heat-capacity anomaly is reduced appreciably from that of four layers. We believe that these features are due to a stronger interlayer coupling right next to the surface ($J_{SV} \gg J_V$). This tends to lock the surface layer to its neighbor. Thus for $n = 4$, provided that J_{SV} is strong enough, all four layers get ordered together, resulting in only one peak in the heat capacity. This accounts for the merging of the peaks for $n = 4$. For $n = 3$, all three layers get locked together, and since there are no weak interlayer bonds, the ordering temperature is suddenly much higher. Such a strong surface coupling J_{SV} is expected because the surface atoms fluctuate much less than their bulk counterparts.

B. Thick films (n > 10)

As n increases the two peaks asymptotically approach a constant separation, and their behavior should be describable by finite-size scaling. In these experiments both $T_S(n)$ and $T_B(n)$ approach their $n \rightarrow \infty$ limit from above. However, according to the general results of finite-size scaling, for a system with open boundary conditions, $T_B(n)$ should approach its asymptotic limit as $1/n^{1/\nu}$ from below (due to the geometrical effect of missing neighbors at the surface). Even neglecting this sign difference, the fitting of the experimental data to the finite-size prediction, $\Delta T \sim 1/n^{1/\nu}$, leads to a value of $\nu = 0.20$. This is both inconsistent with the XY behavior ($\nu \approx \frac{2}{3}$), and with the prediction based on the measured heat-capacity exponent [$\alpha \approx 0.59$ (Ref. 7)] and hyperscaling [$\nu = (2-\alpha)/3 \approx 0.47$]. These facts suggest that although n is quite large, it is not yet large enough to exhibit the usual finite-size scaling, and that there are important preasymptotic behaviors. In fact, we shall show that the true asymptotic limit is only reached for $n \gg \xi_S$, where ξ_S is a new length scale associated with surface ordering. There are indications that in these liquid-crystal films $\xi_S \sim 100$.

III. TWO-DIMENSIONAL ISING MODEL ON FINITE STRIPS

We start by examining the 2D Ising model,[13] which is exactly solvable, and has provided much insight in the context of phase transitions. It has been used for studies of two-dimensional wetting,[14] bond randomness,[15] and frustration.[16] It has also served as a testing ground for scaling theories of critical phenomena. Finite-size effects on two-dimensional Ising models with different boundary conditions have been studied by various authors.[13,17,18] For a strip of finite size, there is no true singularity in the heat capacity, but there is a sharp peak for large n. As $n \rightarrow \infty$, this peak develops into a logarithmic singularity, i.e., $C_V \rightarrow C \ln n$, with C a positive constant, while the peak position $T_B(n)$ shifts to the bulk transition temperature T_C; $\Delta T(n) \equiv T_B(n) - T_C \rightarrow 0$. By general finite-size scaling arguments, we expect $\Delta T \sim b/n$, where b is a constant. The actual value of b depends on several factors: the boundary condition, anisotropy, the shape of the finite geometry, etc. Here we briefly summarize previous results concerning behavior of $T_B(n)$ in strip geometries: Strips with periodic boundary condition, as originally studied by Onsager,[13] indicate $\Delta T \sim a \ln(n)/n^2$, where a is a positive constant. In this case the leading term b/n vanishes. For a strip with open boundary conditions and $J_S = 1$, i.e., no enhancement of surface couplings, $\Delta T \sim b/n$, with $b = -2.025\,818$.[18,19] With open boundary conditions and with a small magnetic field H applied to one boundary, Au-Yang and Fisher[18] obtained $b = 0$, provided that asymptotically $h\sqrt{n} \rightarrow \infty$, with $h = H/k_B T$ the scaling field This result implies a length scale ξ_h associated with h, $\xi_h \sim 1/h^2$, such that as n exceeds ξ_h, the asymptotic shifting of the peak is of higher order.

Here we consider two-dimensional $n \times \infty$ strips with free boundary conditions and strengthened surface couplings. This model is related to that studied by Au-Yang and Fisher[18] via duality. The Hamiltonian is that of (1.1), with S_i^α replaced by Ising spins σ_i^α, and with four different coupling parameters, as indicated in Fig. 1:

$$\mathcal{H} = \sum_i J_S(\sigma_i^1\sigma_{i+1}^1 + \sigma_i^n\sigma_{i+1}^n) + \sum_i J_{SV}(\sigma_i^1\sigma_i^2 + \sigma_i^{n-1}\sigma_i^n)$$
$$+ \sum_{\alpha=2}^{n-1}\sum_i J_H\sigma_i^\alpha\sigma_{i+1}^\alpha + \sum_{\alpha=2}^{n-2}\sum_i J_V\sigma_i^\alpha\sigma_i^{\alpha+1} . \quad (3.1)$$

The partition function is calculated using a mapping from the Ising model to the dimer problem.[20,21] Diagrams in the high-temperature expansion for the Ising model are in one-to-one correspondence with dimer

configurations, and the partition function is obtained by summing over all dimer configurations with appropriate weight. This has an elegant solution in terms of Pfaffians of antisymmetric matrices, which is easily evaluated by computing a determinant.[22] The full expression with four coupling constants is given in Appendix A. The large n asymptotic behavior is captured by the simpler case with $J_{SV} = J_V$, where the expression for the singular part of the free energy per spin reduces to

$$-\beta f_{\text{sing}} = \frac{1}{n}\int_0^1 \frac{d\omega}{\pi\sqrt{1-\omega^2}} \ln(f_+\lambda_+^{n-2} + f_-\lambda_-^{n-2}) , \quad (3.2)$$

where in terms of $Z_1 = \tanh(\beta J_H)$, $Z_2 = \tanh(\beta J_V)$, and $Z_S = \tanh(\beta J_S)$, we have

$$f_\pm = [(1-Z_S)^2 + 4Z_S\omega^2]^2 V_\pm^2 + 16Z_S^2Z_2^2\omega^2(1-\omega^2)V_\mp^2 \pm 8V_+ V_- Z_S Z_2\omega\sqrt{1-\omega^2}[(1-Z_S)^2 + 4Z_S\omega^2] , \quad (3.3)$$

$$V_\pm = \left[\frac{1}{2}\left|1\pm\frac{\sqrt{g}\left[\frac{\tau^2}{n^2} + \frac{\tau}{n}\frac{Z_2(1+Z_1)}{\sqrt{Z_1(1-Z_2^2)}} + \left[\frac{1+Z_2^2}{1-Z_2^2}\right]\omega^2\right]}{\left[\left[\frac{\tau^2}{n^2} + \omega^2\right]g + 1\right]^{1/2}\left[\frac{\tau^2}{n^2} + \omega^2\right]^{1/2}}\right|\right]^{1/2} , \quad (3.4)$$

and

$$\lambda_\pm = 1 + 2g\left[\frac{\tau^2}{n^2} + \omega^2\right]$$
$$\pm 2\left\{\left[\left[\frac{\tau^2}{n^2} + \omega^2\right]g + 1\right]\left[\frac{\tau^2}{n^2} + \omega^2\right]g\right\}^{1/2} . \quad (3.5)$$

Here τ is the scaling variable associated with the reduced temperature,

$$\tau = n\frac{1 - Z_1 - Z_2(1+Z_1)}{2\sqrt{Z_1(1-Z_2^2)}} , \quad (3.6)$$

and g measures bulk anisotropy,

$$g = \frac{\sinh(2\beta J_H)}{\sinh(2\beta J_V)} . \quad (3.7)$$

We first examine the dependence of heat capacity on n numerically. Throughout this paper we use J_H to set the temperature scale, i.e., T is measured in units of J_H/k_B, while all other couplings are measured in terms of J_H. The numerical results are depicted in Figs. 2–7. Figure 2 shows the evolution of heat capacity with increasing n for a stronger surface coupling, $J_S = 2.5$. We observed that initially the position of the maximum, i.e., the peak temperature $T_B(n)$, moves to lower temperature from above T_C. It continues to move below T_C and eventually turns around to approach its asymptotic limit *from below*. The peak position, calculated from a series of different surface couplings J_S, is plotted in Fig. 3. For sufficiently strong surface couplings we always observe an initial decrease in

the peak position before the asymptotic behavior sets in. To understand the scaling behavior, for each J_S we first locate N_t, the number of layers corresponding to the minimum in $T_B(n)$ from Fig. 3. We shall identify N_t with a length scale ξ_S associated with surface ordering. Figure 4 indicates the dependence of N_t upon J_S, and we find that the results are well fitted to

$$\xi_S \equiv N_t \sim \exp\{\delta J_S\} , \quad (3.8)$$

with $\delta \approx 1.87$. We also note from Fig. 3 that strengthen-
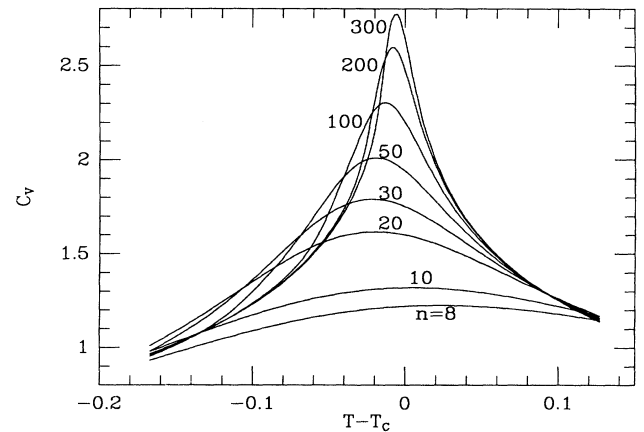

FIG. 2. Heat-capacity curves for Ising models with $J_S = 2.5$ and $J_V = 1$. The number of layers in the strip is varied from 8 to 300.
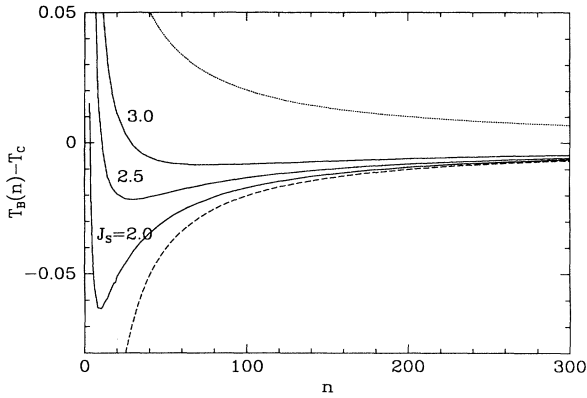
FIG. 3. Variation of the peak position $T_B(n) - T_C$ with the number of layers n. The solid curves correspond to different surface couplings J_S, while the dashed curve indicates the finite-size scaling prediction for $J_S = 1$. The dotted line corresponds to $J_S \rightarrow \infty$. All curves are for $J_V = J_H$.

ing J_S always increases the pseudocritical temperature, i.e., for a given n, $T_B(n)$ is a monotonically increasing function of J_S.

Since the length scale ξ_S is quite large, it is reasonable to expect that some universal function governs the behavior of $\Delta T(n, \xi_S) = T_B(n) - T_C$. The natural scaling variable is $x = n/\xi_S$, and similarly we expect to rescale ΔT by $\xi_S^{1/\nu}$, where ν is the exponent for bulk correlation length. In the 2D Ising model, $\nu = 1$, hence we use $y = \Delta T \xi_S$. Figure 5 indicates that such scaling does indeed lead to a good data collapse and we obtain a scaling function $y = F_S(x)$. This function is obtained in the double scaling limit $n \rightarrow \infty, \xi_S \rightarrow \infty$, while keeping the scaling variable $x = n/\xi_S$ fixed. For $J_S \rightarrow \infty$ and n finite, $\xi_S \rightarrow \infty, x \rightarrow 0$, we obtain the asymptotic behavior of
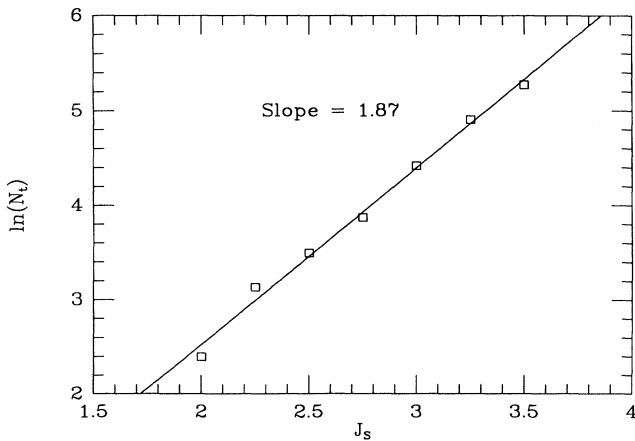
$F_S(x)$ as $x \rightarrow 0$. We will show by a duality argument that $F_S(x) \sim 2.025\,818/x$ as $x \rightarrow 0$, indicated in Fig. 5 by the dotted line. On the other hand, the curve for $J_S = 1$ and large n represents asymptotic behavior for $F_S(x)$ as $x \rightarrow \infty$. From the known results,[18,19] we get $F_S(x) \rightarrow F_\infty(x) \sim -2.025\,818/x$ as $x \rightarrow \infty$, indicated in Fig. 5 by the dashed line. The scaling function we obtained by data collapse approaches the above two asymptotic limits, as can be seen from Fig. 5. For $n \gg \xi_S$, we recover the usual finite-size scaling prediction. However, the deviation is already appreciable at $x \sim 4$, where $F_S(x)$ starts to turn around and be dominated by surface couplings. There is a clear minimum for $x \sim 1$, and for smaller x the peak position decreases with n/ξ_S. Anisotropy of couplings does not change the qualitative behavior. For $J_V/J_H = 0.5$ we found $\xi_S \sim \exp(\delta J_S)$ but with $\delta \approx 2.55$.

The above trends for the surface length scale ξ_S and the scaling function $F_S(x)$ can also be obtained by analyzing the exact expression for the partition function. As far as finite-size scaling is concerned, only the singular part of the free energy is relevant. Following Au-Yang and Fisher,[18] we break the integration in Eq. 3.2 into two parts, $\int_0^1 d\omega = \int_0^{1/\sqrt{n}} d\omega + \int_{1/\sqrt{n}}^1 d\omega$. Since the integrand is singular at the origin ($\omega = 0$) for $\tau = 0$, the dominant contribution to the integral comes from the first term, $\int_0^{1/\sqrt{n}} d\omega$. The surface coupling enters into the expression through f_+ and f_-, and in the large J_S limit,

$$f_\pm \approx 16[\exp(-4\beta J_S) + \omega^2]^2 V_\pm^2 + 16 Z_2^2 \omega^2 (1 - \omega^2) V_\mp^2$$

$$\pm 32 V_+ V_- Z_2 \omega \sqrt{1 - \omega^2} [\exp(-4\beta J_S) + \omega^2] \ . \quad (3.9)$$

By rescaling the integration variable $\rho \rightarrow \omega \sqrt{n}$, we get $\int_0^{1/\sqrt{n}} d\omega \rightarrow \int_0^1 (d\rho/\sqrt{n})$, and $\exp(-4\beta J_S) + \omega^2 \rightarrow (1/n)(x + \rho^2)$. Here $x = n \exp[(-4\beta J_S)]$ is the scaling variable associated with the surface, since the factor

FIG. 4. The turning points N_t in Fig. 3 as a function of the surface coupling J_S in a smilogarithmic plot. The solid line is the fit to the data points.
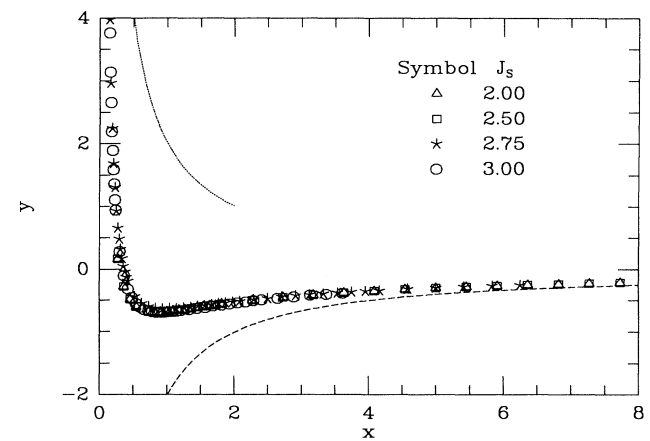

FIG. 5. Data collapse for curves in Fig. 3. Different symbols correspond to different surface couplings. The asymptotic forms of $F_S(x)$ as $x \rightarrow \infty$ and $x \rightarrow 0$ are indicated by the dashed and dotted lines, respectively.

$\exp(-4\beta J_S)+\omega^2$ is the only place that the surface coupling enters into the expression. In analogy to previous results,[10] it is reasonable to assume that the specific heat has the form

$$C \approx A_0 \ln(n) + Q(\tau,x) + O\left[\frac{\ln(n)}{n}\right], \qquad (3.10)$$

where A_0 is a constant independent of the surface coupling. By maximizing the function Q with respect to τ, we get the peak position $\tau_m = G(x)$. Recalling that $\tau \sim n\,\Delta T$, this implies $\Delta T\exp(4\beta J_S) \sim G(x)/x \sim F_S(x)$, i.e., exactly the scaling we obtained from the numerical study. We have not pursued the analytical computation of the function $Q(\tau,x)$. As far as the peak position is concerned, for large n, we can use $\beta=\beta_C$ to identify the coefficient $\delta=4\beta_C$. The results $\beta_C=0.44070$, $\delta=1.7628$ for $J_V=1$, and $\beta_c=0.60938$, $\delta=2.4375$ for $J_V=0.5$ both agree with our numerical studies within a few percent.

As mentioned earlier, our model (model 1) is dual to one with a surface field applied to the two boundary rows (model 2). The low-temperature expansion of model 1 has the same diagrammatic representation as the high-temperature expansion of model 2. (By contrast, Au-Yang and Fisher[18] study a model with the field applied to only one boundary.) To be explicit, we have the following relation between free energies:

$$-\beta f(n,T,J_S) = \frac{n-2}{n}[-\tilde{\beta}\tilde{f}(n-2,\tilde{T},H)], \qquad (3.11)$$

where the parameters are related by the usual dual relations:

$$\tanh(H/\tilde{T}) = \exp(-2J_S/T),$$
$$\tanh(1/\tilde{T}) = \exp(-2/T). \qquad (3.12)$$

It can be shown (see Appendix B) that for large n, if model 1 has a peak at ΔT, then model 2 has a peak at $\Delta\tilde{T}=-\Delta T$ with equal height (both temperature

differences are from T_C, which is the self-dual point). Therefore, we can construct a figure similar to Fig. 3 for model 2 by duality, as shown in Fig. 6. We see that for small h, the peak approaches T_C first from below and asymptotically as b/n from above with $b=2.025818$. It is interesting to compare this figure with the results obtained by Au-Yang and Fisher, with the field applied to only one boundary. They conclude that the peak always approaches T_C from below, and that in the asymptotic region for $h\sqrt{n}\gg1$ the shifting amplitude b is zero. The dual of the method studied by Au-Yang and Fisher has $J_S=\infty$ on one boundary and finite on the other, hence the length scale from one surface has already reached infinity. Despite the difference, we expect the length scales associated with the surface field to have similar scaling. Au-Yang and Fisher discovered a length scale $\xi_h\sim h^\Delta$, with $\Delta=-2$. Through duality relation (3.12), we expect in model 1 a length scale of $\xi_S\sim\exp(4\beta_C J_S)$, in agreement with previous stated numerical and analytical results. The fact that the length scale from one surface is infinite in the model studied by Au-Yang and Fisher probably explains why the turning around behavior is absent in their model. Finally, the usual result for $h=0$ by duality implies that for the model with $J_S=\infty$, ΔT approaches zero *from above* as $2.025818/n$. We thus also have the behavior of the scaling function $F_S(x)\to2.025818/x$ for $x\to0$ (indicated in Fig. 5 with a dotted line).

To compare with experiments of thin films with $n\sim3$–10, we calculated heat capacities for the model with four different couplings using the exact solution in Appendix A. Figure 7 shows the results with one set of suitably chosen parameters ($J_S=2.0$, $J_{SV}=3.0$, $J_V=0.1$). Except for the shape of the peaks, we see that these curves reproduce basically all the qualitative features of the experiments. Shifts of both bulk and surface peaks exhibit the correct trend (towards lower temperatures), with the relative weight of the bulk peak increasing with n. It is crucial that J_{SV} is much stronger
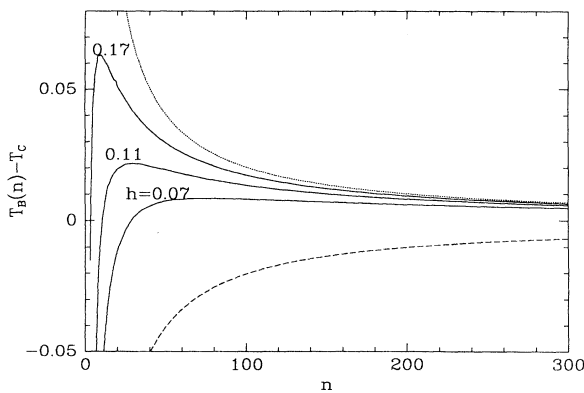

FIG. 6. Peak position as a function of n for different scaled magnetic fields in the dual model (model 2), constructed from Fig. 3 through the duality relation. The dashed line corresponds to the finite-size scaling prediction for $h=0$, while the dotted line corresponds to $h=\infty$.
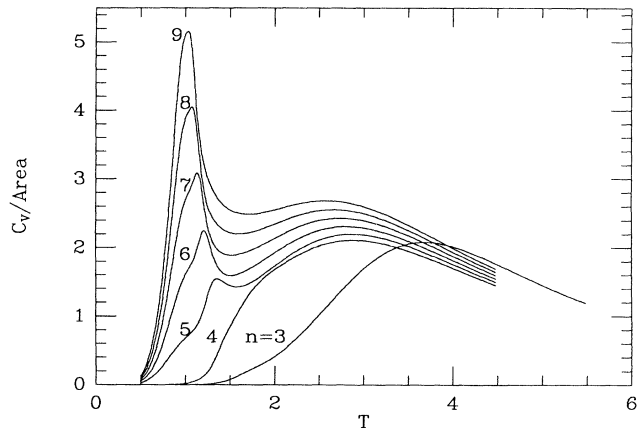

FIG. 7. Heat-capacity curves for thin Ising strips with four couplings; the number of layers vary from 3 to 9. To compare with experiments, the heat capacity is plotted per unit area rather than per spin.

than J_V, so as to account for the merging of the peaks at $n = 4$, and also the jump from $n = 4$ to 3 in the peak position.

IV. MEAN-FIELD THEORY

Another approach to this problem is to study its mean-field behavior, which is usually valid in high dimensions where fluctuations are irrelevant. For large n the problem is similar to semi-infinite systems, which have been extensively studied.[11,23,24,12] The phase diagram is shown in Fig. 8, and crucially depends on two parameters $t = (T - T_C)/T_C$ and g. As usual, t is the reduced temperature, while g is a surface enhancement factor related to the strengthened surface couplings. We now briefly summarize the results.

(a) $g = 0$. As $g \to 0$, the surface length diverges as $\xi_S \sim g^{-1}$. There is only one transition at $t = 0$ (the *special* transition). In this case the magnetization profile is a constant.

(b) $g < 0$. This corresponds to weak surface coupling, and there is only one bulk transition (the *ordinary* transition). Typically, the magnetization profile exponentially increases from a minimum value at the surface towards its bulk value within a length ξ_S (called the *extrapolation length*). The specific heat has one discontinuous jump at the bulk T_C.

(c) $g > 0$. The surface coupling is sufficiently strong, and there are two distinct transitions: a surface ordering transition at T_S and a bulk ordering transition at T_C (the *extraordinary* transition). After the surface orders, we have a magnetization profile that exponentially decays from a maximum value at the surface towards zero in the bulk. The second transition (bulk transition) then changes the bulk magnetization to a nonzero value. The heat capacity has two discontinuous jumps, one at the surface transition T_S (higher temperature) and one at
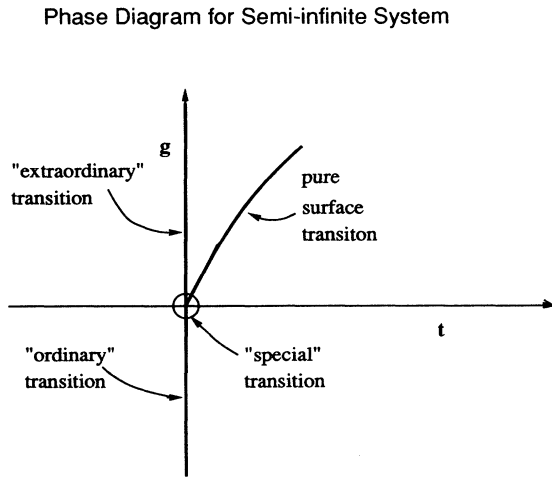
bulk transition T_C (lower temperature). The surface transition temperature increases with g, while the bulk transition temperature is unaffected by the surface coupling g.

We would like to understand how these results are modified by finite-size effects and the strip geometry. To do mean-field theory for layered systems with open boundary conditions and different surface couplings, we determine the magnetization profile $M_\alpha = \langle S_i^\alpha \rangle$, where α denotes the layer index. The M_α are then self-consistently calculated by replacing the couplings to neighboring spins with effective magnetic fields. Since the mean-field results are independent of spin and space dimensionality, we use Ising spins in the layered system on a cubic lattice. The self-consistent equations are

$$M_1 = \tanh[\beta(4J_S M_1 + J_{SV} M_2)] \ ,$$

$$M_2 = \tanh[\beta(4M_2 + J_{SV} M_1 + J_V M_3)] \ ,$$

$$M_3 = \tanh[\beta(4M_3 + J_V M_2 + J_V M_4)] \ ,$$

$$\cdots \ , \tag{4.1}$$

$$M_{n-1} = \tanh[\beta(4M_{n-1} + J_V M_{n-2} + J_{SV} M_n)] \ ,$$

$$M_n = \tanh[\beta(4J_S M_n + J_{SV} M_{n-1})] \ .$$

To study the finite-size effect in the large n limit, we again consider the simpler case of $J_{SV} = J_V$. At high temperatures Eqs. (4.1) have the solution $M_\alpha = 0$ corresponding to the disordered phase. As the temperature is reduced this solution becomes unstable and a nonzero profile describes the minimum free energy. Since the transition is continuous, this instability can be obtained by linearizing the right-hand side. The transition is obtained by requiring that the largest eigenvalue of the matrix of coefficients is unity. The linearization leads to the matrix

Phase Diagram for Semi-infinite System

FIG. 8. Phase diagram of the semi-infinite system in mean-field theory. g is the surface enhancement factor and t is the reduced temperature. The bold lines indicate various phase boundaries.

$$A = \beta \begin{pmatrix} 4J_S & J_V & & & & \\ J_V & 4 & J_V & & & \\ & J_V & 4 & J_V & & \\ & & & \ddots & & \\ & & & J_V & 4 & J_V \\ & & & & J_V & 4J_S \end{pmatrix} . \tag{4.2}$$

Since the eigenvector corresponding to the largest eigenvalue must be symmetric and have positive elements, we assume a form

$$X = \begin{pmatrix} a+b \\ at+bt^{-1} \\ at^2+bt^{-2} \\ \vdots \\ at^2+bt^{-2} \\ at+bt^{-1} \\ a+b \end{pmatrix} . \tag{4.3}$$

It can be checked easily that $AX = \lambda X$, with

$$\lambda = \beta[4 + J_V(t + t^{-1})] \ , \tag{4.4}$$

provided that t is the solution to the following polynomial equation:

$$\frac{t^{n+1}+1}{t^n+t}=\frac{4(J_S-1)}{J_V}\equiv g+1 \; , \tag{4.5}$$

which defines the surface enhancement factor g. The solution of Eq. (4.5) gives us the first transition temperature. The behavior below this temperature requires knowledge of solutions of the coupled nonlinear equations (4.1). The magnetization profile just below this temperature is proportional to the eigenvector X, and its behavior crucially depends on g. There are three distinct behaviors.

(i) $g<0$ corresponds to weak surface coupling. The value of t in Eq. (4.4) is complex and the magnetization is smaller at the surface than in the bulk, i.e., the transition indicates the onset of bulk order. [Magnetization profiles at lower temperatures are indicated in Fig. 9(a).] Setting $t=e^{i\alpha}$, Eq. (4.5) simplifies to

$$(g+1)\cos\left[\frac{n-1}{2}\right]\alpha=\cos\left[\frac{n+1}{2}\right]\alpha \; . \tag{4.6}$$

The solution α closest to zero gives the largest eigenvalue λ_n. Setting $\lambda_n=1$ determines the transition temperature $T_B(n)$ which in the $n\to\infty$ limit behaves as

$$T_B(n)=4+2J_V-J_V\frac{\pi^2}{n^2}-2J_V\frac{\pi^2}{n^2}\frac{g+2}{ng}+O\left[\frac{1}{n^4}\right] \; . \tag{4.7}$$

The bulk transition approaches its asymptotic limit $T_C=4+2J_V$ from below; the leading correction scales as $1/n^2$ ($v=\frac{1}{2}$) with a coefficient that is independent of surface coupling. We can also include the $1/n^3$ term into a scaling form, $\Delta T_B(n)=1/n^2 f(n/\xi_S)$ with $\xi_S\equiv 1/g$.

(ii) With $g=0$, $t=1$ and the magnetization profile below T_C is uniform. This special transition is not modified by finite-size effects, i.e., $T_B(n)=T_C$ for all n. In cases (i) and (ii) the heat capacity exhibits a single jump at T_C.

(iii) For $g>0$, the surface couplings are sufficiently strong to produce surface ordering before the bulk. Typical magnetization profiles are shown in Fig. 9(b) and indicate a decay of the magnetization into the bulk. Just below the transition, as seen from the eigenvector in Eq. (4.3), the magnetization decays as $t^n\sim\exp(-n/\xi_S)$, with $t\sim 1-1/\xi_S\sim(1+g)^{-1}$ from Eq. (4.5). The heat capacity exhibits a discontinuity at this instability temperature $T_S(n)$. Upon further cooling the profile changes continuously, but due to finite thickness a sharp bulk transition is absent. One can, however, still define a position $T_B(n)$ for the second peak in heat capacity that approaches T_C as $n\to\infty$.

Solutions of the linearized equations again provide us with the finite-size dependence of the surface transition temperature, and we find

$$T_S(n)=4+(1+g)J_V+\frac{J_V}{1+g}$$
$$+J_V(1+g)^{-n+2}+O((1+g)^{-n+1}) \; . \tag{4.8}$$

As $n\to\infty$, $T_S(n)\to T_S=4+(1+g)J_V+J_V/(1+g)$, which reproduces the phase diagram in Fig. 8. Again, we introduce a surface length scale $\xi_S\equiv 1/\ln(1+g)$ in terms of which Eq. (4.8) can be rewritten as

$$T_S(n)=T_S+J_V(1+g)^2\exp(-n/\xi_S) \; . \tag{4.9}$$

The surface transition exponentially decays to its semi-infinite limit from above, with a decay length set by ξ_S.

The study of the finite-size effects on the bulk peak requires much more work. This is because in a finite-size system there is no sharp discontinuity and the heat capacity is rounded off at the pseudocritical temperature
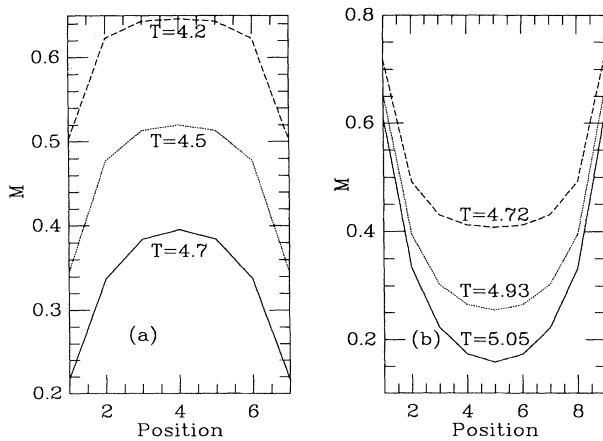

FIG. 9. (a) A typical magnetization profile for $g<0$ with $n=7$, $J_S=1$, and $J_{SV}=J_V=0.5$. The bulk transition temperature is at $T_B(n)=4.9239$. (b) A typical magnetization profile for $g>0$ with $n=9$, $J_S=1.4$, and $J_{SV}=J_V=0.5$. The surface transition temperature is $T_S(n)=5.7564$. Points are connected to guide the eyes.
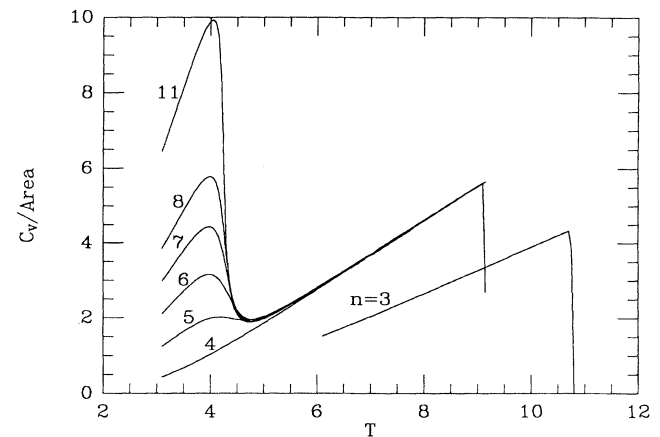

FIG. 10. Heat-capacity curves for the model with four couplings in mean-field theory. The number of layers varies from 3 to 11.

$T_B(n)$. Thus the behavior can only be studied numerically by solving the nonlinear equations. We developed a program to solve the full set of equations (4.1) on the computer. The resulting magnetization profile was used to compute the energy and heat capacity. Some typical heat-capacity curves are shown in Fig. 10. We see that in addition to the sharp singularity at $T_S(n)$, there is a rounded off anomaly at a lower temperature $T_B(n)$ which evolves into the bulk discontinuity as $n \to \infty$. The position of the peak as a function of n is plotted in Fig. 11 for three different surface couplings. As in the two-dimensional system, $T_B(n)$ has a nonmonotonous dependence on n (initially deceasing with n, and eventually approaching its limiting value from below). Note that, unlike the $d = 2$ case, $T_B(n)$ in Fig. 11 *decreases* as the surface coupling is increased. However, in this case ξ_S is also a decreasing function of J_S so that dependence of $T_B(n)$ with ξ_S is similar to $d = 2$.

The data in Fig. 11 can also be collapsed upon appropriate rescaling of the axes. By analogy with $d = 2$ we expect $\Delta T_B(n, \tilde{\xi}_S) = \tilde{\xi}_S^{-1/\nu} F_S(n / \tilde{\xi}_S)$, where $\nu = \frac{1}{2}$ in the mean-field theory. [This can be obtained by minimizing $C(nt^\nu, n / \tilde{\xi}_S)$ to obtain a peak at $t = 1/n^{1/2} f(n / \tilde{\xi}_S)$.] The length scale $\tilde{\xi}_S$ is obtained directly from the measured collapse of the magnetization profile and is in fact different from ξ_S calculated earlier at the surface transition due to nonlinear corrections. The resulting scaling function is indicated in Fig. 12 and has the same qualitative behavior as the result for $d = 2$, although the exponent ν is different. For large n, $F_S(x) \to a / x^2$ with a a negative constant.

In order to compare with the experiments on thin films, we calculated heat capacities for n varying from 3 to 11 using four suitably chosen interactions. The results are plotted in Fig. 10, and again, the additional coupling J_{SV} is necessary to reproduce the behavior of thin-film experiments [7]. For $n > 4$, we see the two typical peaks with the relative weight of the bulk peak increasing with n. For sufficiently strong J_{SV}, the two peaks merge at $n = 4$, and the surface transition temperature jumps significantly from $n = 4$ to 3. All these qualitative
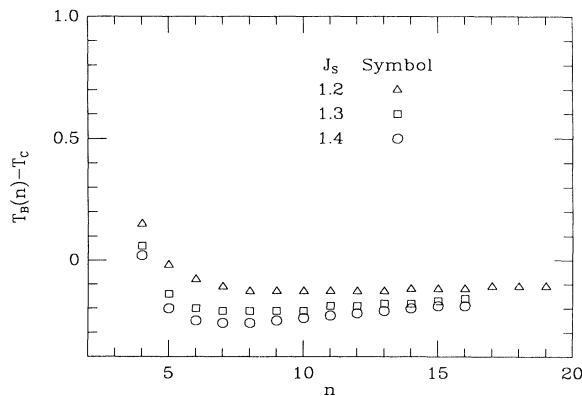
FIG. 11. Peak positions as a function of n in mean-field theory. The different symbols correspond to different surface couplings, and $J_V = 0.5$.
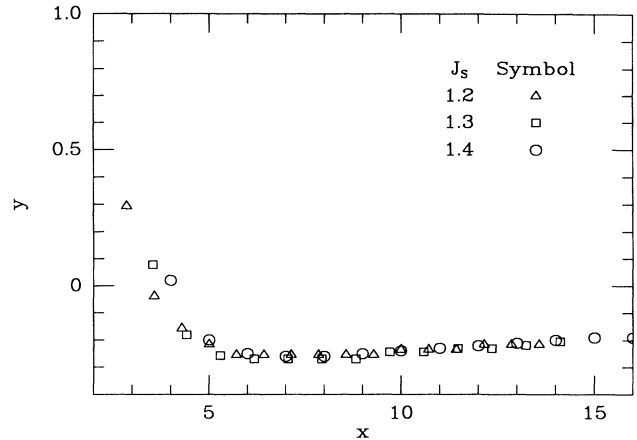
FIG. 12. Data collapse for the curves in Fig. 11.

features are similar to the 2D Ising model case, and are in qualitative agreement with experiments.

V. CONCLUSIONS

We have studied layered systems with strengthened surface couplings both in 2D (Ising model with strong fluctuation) and in mean-field theory (no fluctuations). Both approaches reveal two peaks in the heat capacity corresponding to the onset of surface and bulk ordering. Finite-size scaling behavior is determined by a length scale ξ_S associated with the surface coupling. In the thick-film limit, the surface peak approaches its limiting position from above, while $T_B(n)$ first decreases and then increases to approach T_C from below, following a new scaling function of n / ξ_S. Since this is true in both cases, we believe that the behavior is generic to all models. A more appropriate model for the experimental system is the layered XY model. It is known from analytical work[2] that the 2D XY model possesses no heat-capacity singularity at its transition. However, experiments carried out on thin films as well as Monte Carlo simulations reveal sharp peaks in the heat capacities. This is a problem that is still unresolved. Our recent Monte Carlo simulations on the layered XY model with strengthened surface couplings also reveal two peaks in heat capacity with shifting trends similar to that in the Ising and the mean-field cases.[25] Comparing with experiments, we speculate that $\xi_S \sim 100$ for liquid-crystal films, so that present experimental results are still in the preasymptotic region where only a decrease of $T_B(n)$ with n is observed. For thin films where we do not expect any universal scaling, we can reproduce heat-capacity curves in qualitative agreement with experiments by using a strengthened interlayer coupling at the surface. It would be interesting to determine $F_S(x)$ analytically for general spin models. Also, we would like to understand how different boundary operators change the asymptotic amplitudes, as exhibited in the Ising example.

Note added. After this paper was accepted for publication, we learned that recent experiments have confirmed the predicted nonmonotonic behavior of $T_B(n)$.[9]

ACKNOWLEDGMENTS

APPENDIX A: EXACT SOLUTION FOR THE ISING MODEL WITH FOUR COUPLINGS

In this appendix we give the full expression for the partition function of the Ising model with four couplings on the strip geometry in Fig. 1. With the additional coupling J_{SV}, the full expression is

$$-\beta f = -\beta f_{\text{sing}} + \frac{2}{n}\ln\cosh(J_S\beta) + \frac{2}{n}\ln\cosh(J_H\beta)$$
$$+ \frac{n-2}{2n}\ln\cosh(J_V\beta) + \frac{2}{n}\ln\cosh(J_{SV}\beta)$$
$$+ \frac{n-4}{2n}\ln\sinh(J_V\beta) . \tag{A1}$$

The singular part of the free energy is given by

$$-\beta f_{\text{sing}} = \frac{1}{n}\int_0^1 \frac{d\omega}{\pi\sqrt{1-\omega^2}}\ln(F_+\lambda_+^{n-4}+F_-\lambda_-^{n-4}) . \tag{A2}$$

This expression is similar to the expression in Eq. (3.2), except for a difference in powers of $\lambda_\pm$, and with $F_\pm$ replacing $f_\pm$. Here $\lambda_\pm$ are defined as in Eq. (3.5), and $F_\pm$ are given by

$$F_\pm = D_2^2 V_\pm^2 \pm 2V_+ V_- E_2 D_2 + E_2^2 V_\mp^2 , \tag{A3}$$

with $V_\pm$ the same as in Eq. (3.4). E_2 and D_2 have the following expressions:

$$D_2 = [(1-Z_1)^2+4Z_1\omega^2][(1-Z_S)^2+4Z_S\omega^2]$$
$$+ 16Z_S Z_1 Z_{SV}^2\omega^2(1-\omega^2) , \tag{A4}$$
$$E_2 = -4\omega\sqrt{1-\omega^2}\{Z_1 Z_2[(1-Z_S)^2+4Z_S\omega^2]$$
$$+ Z_2 Z_S Z_{SV}^2[(1+Z_1)^2-4Z_1\omega^2]\} . \tag{A5}$$

The parameters Z_1, Z_2, and Z_S are given as before while the new parameter Z_{SV} is given by $Z_{SV}=\tanh(\beta J_{SV})$.

APPENDIX B: DUALITY RELATIONS

In this appendix, we prove that in the large n limit, if the heat capacity of model 1 has a peak at ΔT, then the corresponding dual model (model 2) will have a peak at $\Delta\widetilde{T}=-\Delta T$ with equal height. We will use C^1 and C^2 to denote heat capacities for models 1 and 2, respectively.

Starting with the duality relation in Eq. (3.11), take two derivatives with respect to T to obtain the following relation [for large n, $(n-2)/n\approx 1$]:

$$C^1(n,T,J_S) = -T\frac{\partial^2 f}{\partial^2 T} \approx -T\frac{\partial^2}{\partial T^2}\left[\frac{T}{\widetilde{T}}\widetilde{f}(n-2,\widetilde{T},H)\right] . \tag{B1}$$

The parameters $\widetilde{T}$ and H in the dual model are related to T and J_S through relations (3.12). Using the chain rule for differentiation, we have

$$\frac{\partial^2}{\partial T^2} = \frac{\partial^2\widetilde{T}}{\partial T^2}\frac{\partial}{\partial\widetilde{T}} + \frac{\partial^2 H}{\partial T^2}\frac{\partial}{\partial H} + \left[\frac{\partial\widetilde{T}}{\partial T}\right]^2\frac{\partial^2}{\partial\widetilde{T}^2}$$
$$+ \left[\frac{\partial H}{\partial T}\right]^2\frac{\partial^2}{\partial H^2} + 2\frac{\partial H}{\partial T}\frac{\partial\widetilde{T}}{\partial T}\frac{\partial}{\partial H}\frac{\partial}{\partial\widetilde{T}} . \tag{B2}$$

Note that in the 2D Ising model there is no singularity in the first derivatives of the free energy, and we only consider the second derivatives in the last three terms of the above equation. The last two terms contain second derivatives of $\widetilde{f}$ with respect to the boundary field, which are not singular when $H\neq 0$ [this is true for any finite J_S through relation (3.12)]. Hence, the only singular term is the second derivative with respect to $\widetilde{T}$, and in the limit $n\to\infty$ we have

$$C^1(n,T,J_S) \approx -T\left[\frac{\partial\widetilde{T}}{\partial T}\right]^2\frac{\partial^2}{\partial\widetilde{T}^2}\left[\frac{T}{\widetilde{T}}\widetilde{f}(n-2,\widetilde{T},H)\right] . \tag{B3}$$

Again, we only keep the term corresponding to second derivative of $\widetilde{f}$, and the above equation reduces to

$$C^1(n,T,J_S) \approx \frac{T^2}{\widetilde{T}^2}\left[\frac{\partial\widetilde{T}}{\partial T}\right]^2\left[-\widetilde{T}\frac{\partial^2}{\partial\widetilde{T}^2}\widetilde{f}(n-2,\widetilde{T},H)\right] . \tag{B4}$$

Since the quantity in the large parentheses is $C^2(n-2,\widetilde{T},H)$, we get the following relation for the singular part of the heat capacities of models 1 and 2:

$$C^1(n,T,J_S) \approx \frac{T^2}{\widetilde{T}^2}\left[\frac{\partial\widetilde{T}}{\partial T}\right]^2 C^2(n-2,\widetilde{T},H) . \tag{B5}$$

As $n\to\infty$, the heat-capacity peak approaches T_C, and we can evaluate the coefficient at T_C. Since the Ising model is self-dual, $T_C=\widetilde{T}_C$, and from Eq. (3.12) we obtain

$$\frac{\partial\widetilde{T}}{\partial T}\bigg|_{T_C} = -1 . \tag{B6}$$

We therefore conclude that if model 1 has a peak at T, then model 2 has a peak at $\widetilde{T}$ with the same height. Using relation (B6), if the peak in model 1 is ΔT away from T_C, then the peak in model 2 is $\Delta\widetilde{T}$ away from T_C with $\Delta\widetilde{T}=-\Delta T$. For the special case $J_S=\infty$, $H=0$ and does not depend on T. Still there are no contributions from the last two terms in Eq. (B2), and hence the above conclusion based on Eq. (B5) is still valid.

[1]D. J. Bishop and J. Reppy, Phys. Rev. Lett. **40**, 1727 (1978).

[2]J. M. Kosterlitz and D. J. Thouless, J. Phys. C **6**, 1181 (1973).

[3]D. R. Nelson and J. M. Kosterlitz, Phys. Rev. Lett. **39**, 1201 (1977).

[4]R. Birgeneau and D. Lister, J. Phys. (Paris) Lett. **39**, 399 (1978); M. Cheng, J. T. Hu, S. W. Hui, and R. Pindak, Phys. Rev. Lett. **61**, 550 (1988).

[5]D. R. Nelson and B. I. Halperin, Phys. Rev. B **19**, 2457 (1979).

[6]D. J. Tweet, R. Holyst, B. D. Swanson, H. Stragier, and L. B. Sorensen, Phys. Rev. Lett. **65**, 2157 (1990).

[7]R. Geer, C. C. Huang, R. Pindak, and J. W. Goodby, Phys. Rev. Lett. **63**, 540 (1989).

[8]R. Geer, T. Stoebe, C. C. Huang, R. Pindak, G. Srajer, J. W. Goodby, M. Cheng, J. T. Ho, and S. W. Hui, Phys. Rev. Lett. **66**, 1322 (1991).

[9]C. C. Huang (private communication).

[10]For a review, see M. Barber, in *Phase Transitions and Critical Phenomena*, edited by C. Domb and J. L. Lebowitz (Academic, London, 1983), Vol. 8.

[11]For a review, see K. Binder, in *Phase Transitions and Critical Phenomena* (Ref. 10).

[12]H. Nakanishi and M. Fisher, Phys. Rev. Lett. **49**, 1565 (1982).

[13]L. Onsager, Phys. Rev. **65**, 117 (1944).

[14]For a review, see D. B. Abraham, in *Phase Transitions and Critical Phenomena*, edited by C. Domb and J. L. Lebowitz (Academic, London, 1986), Vol. 10.

[15]B. M. McCoy and T. T. Wu, Phys. Rev. **176**, 631 (1968).

[16]M. Kardar and A. N. Berker, Phys. Rev. B **26**, 219 (1982).

[17]A. E. Ferdinand and M. E. Fisher, Phys. Rev. **185**, 832 (1969).

[18]H. Au-Yang and M. E. Fisher, Phys. Rev. B **11**, 3469 (1975).

[19]M. E. Fisher, in *Critical Phenomena, Proceedings of the 51st Enrico Fermi Summer School, Varenna, Italy,* edited by M. S. Green (Academic, New York, 1971).

[20]P. W. Kasteleyn, J. Math. Phys. **4**, 287 (1963).

[21]H. N. V. Temperley and M. E. Fisher, Philos. Mag. **6**, 1061 (1961).

[22]B. McCoy and T. T. Wu, *Two-Dimensional Ising Model* (Harvard University Press, Cambridge, 1973).

[23]K. Binder and P. C. Hohenberg, Phys. Rev. B **6**, 3461 (1972); **9**, 2194 (1974).

[24]T. C. Lubensky and M. H. Rubin, Phys. Rev. B **12**, 3885 (1975).

[25]Hao Li, Mehran Kardar, and Kerson Huang (unpublished).